Revista Brasileira de Geofísica
RBGf
Brazilian Journal of Geophysics

Revista Brasileira de Geofísica (2012) 30(4): 473-482

ISSN 0102-261X
www.scielo.br/rbg

STEREOTOMOGRAPHY FOR VELOCITY MODEL ESTIMATION IN SEISMIC IMAGING: APPLICATION TO REAL DATA FROM JEQUITINHONHA SEDIMENTARY BASIN

Felipe A. Terra[1], Jessé C. Costa[2] and Amin Bassrei[3]

Recebido em 9 novembro, 2010 / Aceito em 11 outubro, 2011
Received on November 9, 2010 / Accepted on October 11, 2011

ABSTRACT. Seismic imaging in depth is a challenge in geologically complex areas, where the seismic velocity varies laterally. The estimation of a reliable velocity model is necessary in order to succeed in seismic depth imaging. Stereotomography is an effective tool to achieve this purpose. Also called slope tomography, it uses the slowness and picked traveltimes from reflection events picked in common source and common receiver gathers. We evaluate an alternative implementation of stereotomography for velocity model building. The algorithm was validated in the Marmousoft synthetic data set and also used for velocity model estimation in a continental slope region, using real data from Jequitinhonha Basin, Brazil. This data set of structural complexity demanded a high quality control of event selection for picking, judicious choice of regularization parameters and free surface multiple attenuation. The results for both the synthetic and real data have shown the computational feasibility and accuracy of this method.

Keywords: stereotomography, regularization, Jequitinhonha Basin.

RESUMO. O imageamento sísmico em profundidade é um desafio em áreas geologicamente complexas, onde a velocidade sísmica apresenta variação lateral. Porém, para se obter sucesso no imageamento sísmico em profundidade é necessário que se tenha uma estimativa confiável do modelo de velocidade. A estereotomografia é uma ferramenta efetiva para se alcançar esse propósito. Também denominada de tomografia de inclinação, ela utiliza as vagarosidades e os tempos de trânsito selecionados de famílias de fonte comum e de receptor comum. Nós avaliamos uma alternativa da estereotomografia para a construção do modelo de velocidades. O algoritmo foi validado no conjunto de dados sintéticos Marmousoft e também em dados reais provenientes da Bacia do Jequitinhonha, Brasil, numa região de talude continental. Este conjunto de dados com complexidade estrutural demandou um controle de alta qualidade na seleção de eventos, numa escolha criteriosa dos parâmetros de regularização, e a atenuação de múltiplas de superfície livre. Os resultados tanto para os dados sintéticos como para os reais mostraram a viabilidade computacional e precisão do método.

Palavras-chave: estereotomografia, regularização, Bacia do Jequitinhonha.

[1]Petróleo Brasileiro S.A., Av. ACM, 1113, Anexo 3, Sala H, AQT/OST, Itaigara, 41830-900 Salvador, BA, Brazil. Phone: +55 (71) 3348-2166 – E-mail: felipeterra@petrobras.com.br

[2]Faculdade de Geociências da Universidade Federal do Pará, Rua Augusto Correa, 1, Guamá, 66075-110 Belém, PA, Brazil. Phone: +55 (91) 3201-7692 – E-mail: jesse@ufpa.br

[3]Instituto de Geociências da Universidade Federal da Bahia, Rua Barão de Jeremoabo, s/n, Ondina, 40170-115 Salvador, BA, Brazil. Phone: +55 (71) 3283-8508 – E-mail: bassrei@ufba.br

INTRODUCTION

The velocity macro-model determination constitutes a crucial step for the seismic imaging of the structural framework on subsurface. The seismic imaging in depth methods require a considerably accurate knowledge of propagation velocity field of seismic waves. In turn, to establish a velocity model related to depth is a costly and laborious task. A common example is the construction of the velocity field in depth using migration velocity analysis techniques, which besides having a high computational cost of the migration, demands elevated processing time to analyze the velocities and define the horizons. In this work, we evaluate an alternative approach, which is to use the stereotomography as an inversion method for the velocity macro-model estimative, aiming in this context to have a minimal human interference and considerable fast process.

This work is also based on a reformulation of the original work of Sword (1986) on a global formulation of the slope tomography (Billette & Lambaré, 1998). The development of stereotomography is based on the general structures of the paraxial ray theory (Cervený et al., 1977; Farra & Madariaga, 1987), Hamiltonian formulation of ray theory (Farra & Madariaga, 1987; Lambaré et al., 1996), and in general inverse problem theory (Tarantola, 1987).

In the slope tomographic methods, besides the traveltime, locally coherent event slopes are also used by the tomographic procedure. The picking of these data was carried out using an automatic selection algorithm (Billette & Lambaré, 1998) and the inversion of them using the algorithm implemented by Costa et al. (2008). With experience in the practical aspects of algorithms, developed in the Marmousoft synthetic datum applications, we extended the method to apply it to a real datum which consists of a marine 2D line of Jequitinhonha Basin, where we confronted peculiar difficulties: data conditioning, attenuating the multiples, and selection of the best pick set for the velocity field estimation.

STEREOTOMOGRAPHY METHOD

Different from the conventional tomography, besides the traveltime picking, the method requires the local slope associated to the selected events, in the common-shot and common-receiver gathers simultaneously. The traveltime picking is well-known and regularly used, unlike the slope picking. A local slope, at a given time, is obtained from a coherence panel (semblance) in the t-p domain (Billette et al., 2003). With a reference trace, a local stack is formed, as Figure 1 shows. At each time, the stack is calculated with different slope values, generating the semblance panel, where the highest coherence values of each trace of common source and common receiver families are automatically selected, where the P_{RX} and P_{SX} values are respectively estimated.

The data consist of a discreet collection of: (i) shot and receiver positions, denoted by S and R, respectively; (ii) two-way traveltime (T_{RS}) and (iii) local slopes of the selected reflected events, expressed by the event slope in the common receiver section, $P_{SX} = \partial T_{SR}/\partial S$, and by the corresponding slope of the event in the common source section, $P_{RX} = \partial T_{SR}/\partial R$). Then, each event in the data space is specified by the following attribute vector:

$$\mathbf{d} = \left[\left[\left(S,\, R,\, P_{SX},\, P_{RX},\, T_{SR}\right)_i\right]_{i=1}^{N}\right]. \qquad (1)$$

The model space is characterized by the model parameter vector $\mathbf{m}$,

$$\mathbf{m} = \left[\left[\left(\mathbf{X},\, \theta_S,\, \theta_R,\, T_S,\, T_R\right)_i\right]_{i=1}^{N}, \left[C_j\right]_{j=1}^{J}\right], \qquad (2)$$

which includes the velocity field C and $6N$ parameters associated to the two ray segments that connect the scatter point to the source and to the receiver, as it is illustrated in Figure 2. That is, the event is modeled as the result of a single diffraction or reflection at some location in depth. In this notation, the pair of ray segments is described by: (i) a common starting point X, (ii) two takeoff angles, Θ_S and Θ_R; and (iii) two one-way traveltimes, T_S and T_R. It is important to point out that the number of parameters m required to describe the model increases with the number of selected events. For large size applications, this increases the computational cost. By perturbing the model parameters using linear approximations, the data are iteratively adjusted in the stereotomography algorithm (Billette & Lambaré, 1998).

The direct problem is non-linear and it is expressed by the functional relationship

$$\mathbf{d} = g(\mathbf{m}), \qquad (3)$$

where the $\mathbf{d}$ and $\mathbf{m}$ vectors were defined before. This relation does not allow the inverse problem having a single and stable solution. For this, it is necessary to add more restrictions to the admissible solution class. In this work, we used an objective function minimized by the classical rule l_2, according to the algorithm implemented in Costa et al. (2008):

$$\begin{aligned}\Phi(\mathbf{m}) = &\left\|\mathbf{d}^{obs} - g(\mathbf{m})\right\|_2^2 + \lambda_{Lap}^2 \left\|(\mathbf{D}_1^2 + \mathbf{D}_1^2)(\mathbf{m} - \mathbf{m}_0)\right\|_2^2 \\ &+ \lambda_{C1}^2 \left\|(\mathbf{D}_1^2(\mathbf{m} - \mathbf{m}^0)\right\|_2^2 + \lambda_{C3}^2 \left\|(\mathbf{D}_3^2(\mathbf{m} - \mathbf{m}_0)\right\|_2^2 \\ &+ \lambda_{G1}^2 \left\|(\mathbf{D}_1(\mathbf{m} - \mathbf{m}_0)\right\|_2^2 + \lambda_{G3}^2 \left\|(\mathbf{D}_3(\mathbf{m} - \mathbf{m}_0)\right\|_2^2 \\ &+ \lambda_R^2 \left\|(\mathbf{D}_R(\mathbf{m} - \mathbf{m}_0)\right\|_2^2 + \lambda_D^2 \left\|(\mathbf{D}_3(\mathbf{m} - \mathbf{m}_0)\right\|_2^2,\end{aligned} \qquad (4)$$

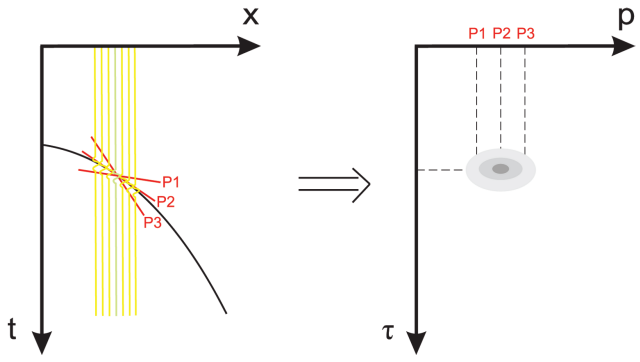

Figure 1 – Data selection scheme using coherence map.

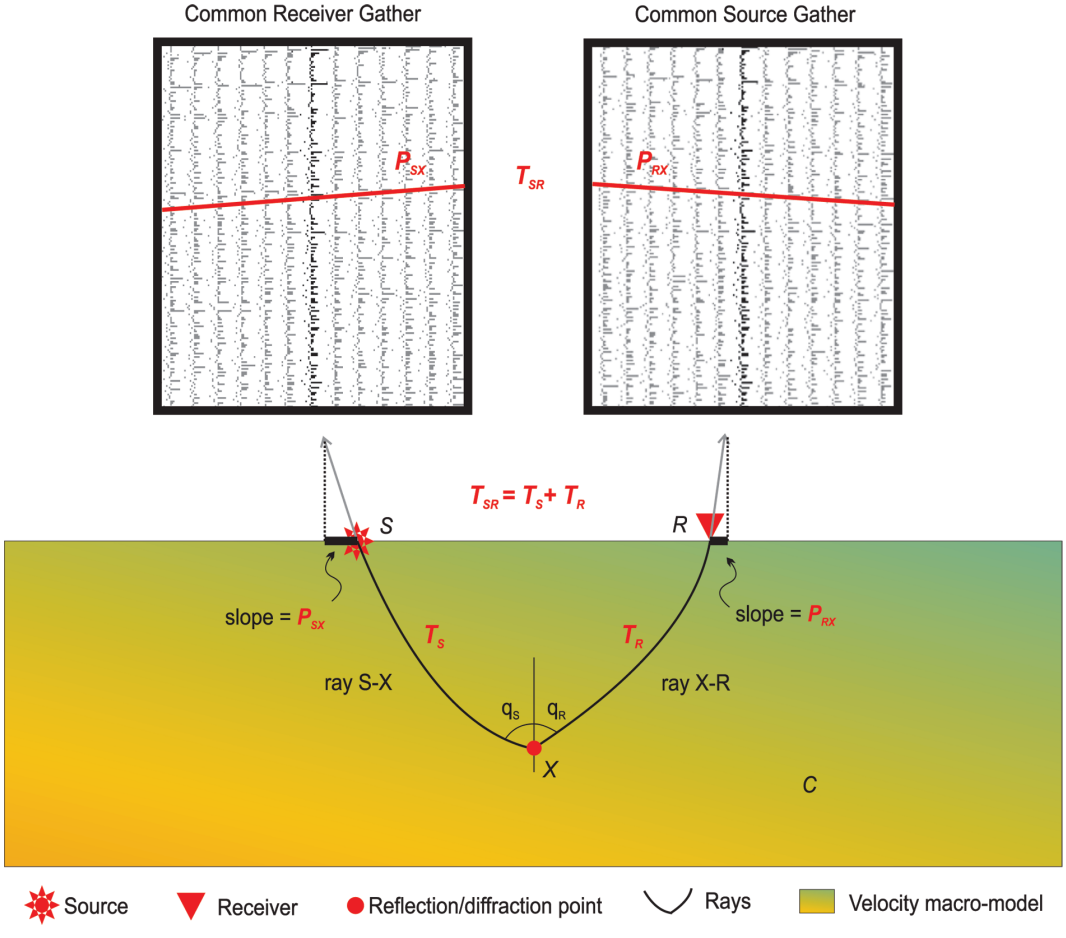

Figure 2 – Illustrative scheme of acquisition in stereotomography with the associated dips of a given coherent event in data space and model space.

where the parameters λ_s act as Lagrange multipliers that ponderate the respective regularization contributions in the objective function. The parameter λ_D acts in all model parameters and its aim is to ponderate their updates, and the parameter λ_R controls the smoothing degree along the reflector. In turn, the parameter λ_{Lap}, related to the Laplacian operator, determines the isotropic curvature smoothing. Finally, the parameters $\lambda_{C1}, \lambda_{C3}, \lambda_{G1}$ and λ_{G3} determine, respectively, the curvature and the gradient in relation to directions x_1 (horizontal) and x_3 (vertical). For more details, see Costa et al. (2008).

The functional minimization 4 is carried out through linear iterations, requiring equation 3 linearization for each iteration:

$$\mathbf{d}^{k+1} - \mathbf{d}^{k} = \frac{\partial g}{\partial \mathbf{m}}|_{\mathbf{m}=\mathbf{m}^{k}}(\mathbf{m}^{k+1} - \mathbf{m}^{k}), \qquad (5)$$

or in a more compact notation,

$$\delta \mathbf{d}^{k} = G^{k} + \delta \mathbf{m}^{k}, \qquad (6)$$

where k represents the iteration number and

$$G^{k} = \frac{\partial g}{\partial \mathbf{m}}|_{\mathbf{m}=\mathbf{m}^{k}}$$

represents the approximation around model $\mathbf{m}^{k}$. The operator G^{k} is a matrix with the derivatives of data parameters with respect to model parameters, called Fréchet derivative.

To obtain the perturbation vector of the model parameters, denoted by $\delta \mathbf{m}^{k}$, it is necessary to linearize all other parcels of the objective function. The resulting linear system (Billette & Lambaré, 1998; Costa et al., 2008) is solved using the conjugate-gradient method LSQR (Paige & Saunders, 1982). Formally, this solution is represented by a generalized inverse $G^{k,+}$, so that

$$\delta \mathbf{m}^{k} = G^{k,+}\delta \mathbf{d}^{k}. \qquad (7)$$

After calculating the parameter perturbation indicated above, the reference model is updated according to the expression

$$\mathbf{m}^{k+1} = \mathbf{m}^{k} + \delta \mathbf{m}^{k}. \qquad (8)$$

In this iterative process, the new data calculated $\mathbf{d}^{cal}$ for $\mathbf{m}^{k+1}$ is estimated and, again, the data adjustment is evaluated. If the adjustment rule $\|\delta \mathbf{d}^{k}\|$ is not smaller than a predetermined value or when it reaches the maximum number of iterations, the equation (5) system is resolved again to a new parameter update according to equation (7).

To initialize the algorithm, two rays are propagated from top to bottom in an initial velocity model, from the source and receiver position. The ray tracing is interrupted when the sum of the two traveltimes of each segment $(T_R + T_S)$ is equal to the event traveltime (T_{RS}). Following, the midpoint between the extremities of each ray segment is determined. This point, then, is considered as an initial approximation for the reflection point X. The angles Θ_S and Θ_R are obtained from the final direction of the extremities that each segment forms with the vertical. In general, the initial model of the model velocities is not correct, so that the calculated positions, slopes and traveltimes will not fit the observed data d^{obs}.

SYNTHETIC EXAMPLE

Initially, we evaluated the method using Marmousoft data, adapted from 2D Marmousi synthetic data by Billette & Lambaré (1998) using ray modeling with Born approximation, which provides a data set free from multiples and refractions. Besides, Marmousoft is a combination of a smoothened velocity field and a very complex reflectivity, as we can observe in Figures 3a and 4a which are the exact velocity field and prestack depth migration result, respectively. All this implies ideal data to evaluate the stereotomography in which the picking step will not be influenced by the multiple reflections and the data itself was originated from the modeling of a smooth velocity field, facilitating the comparison with the estimated models that are also smoothened fields due to the regularizations.

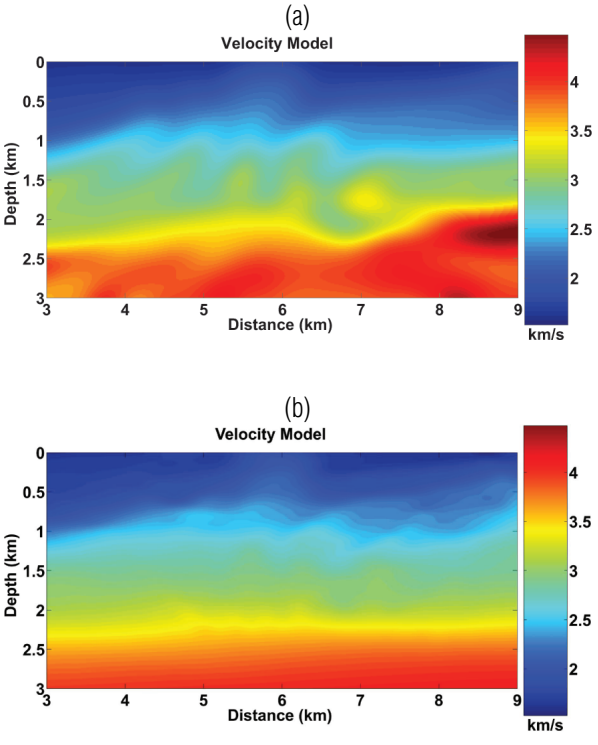

Figure 3 – Velocity model: (a) exact (Marmousoft) and (b) estimated (stereotomography).

The first process step was collecting the picks using the automatic selection tool, which provided a total of 5490 locally coherent events, containing source and receiver positions, traveltime estimations and horizontal slowness components (slopes measured in the events). The following step, which is the data inversion, is initially carried out in a sparse B-spline grid, with 11×11 nodes. They are spaced 1 km laterally and 0.5 km vertically. The result of this inversion is the initial model for the final inversion in a dense B-spline grid, with 51×51 nodes spaced

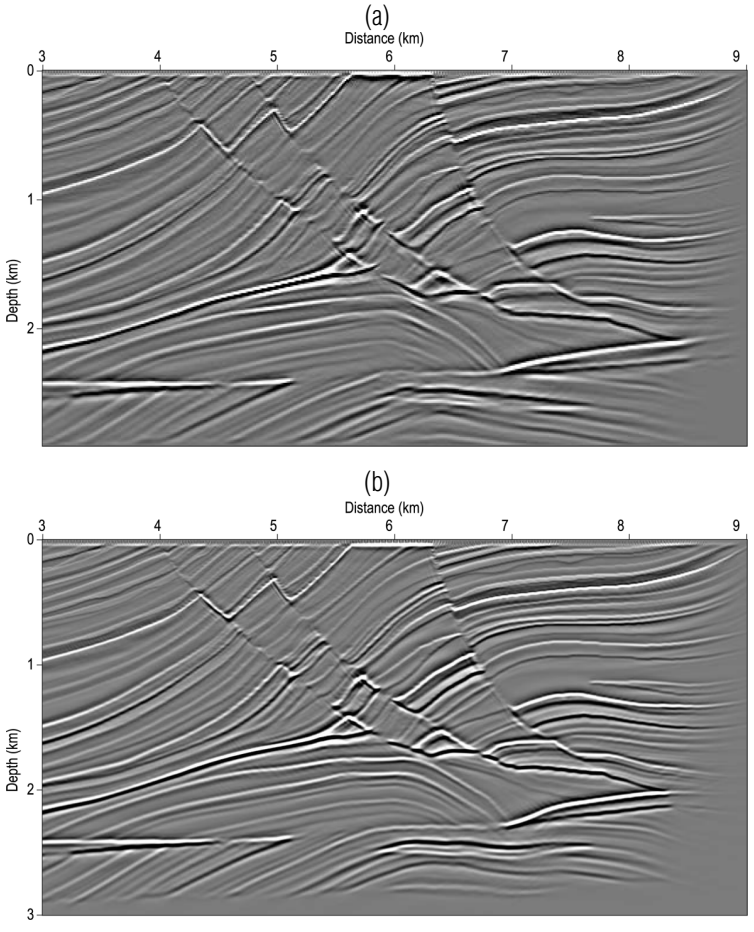

Figure 4 – Migrated field with: (a) exact velocity model (Marmousoft) and (b) estimated velocity model (stereotomography).

0.2 km laterally and 0.1 km vertically. The velocity models are presented after reaching the maximum number of 30 iterations and they are resampled using the 1001 $\times$ 601 grid, where the nodes are spaced 10 m laterally and 5 m vertically, in order to be used in the migration. We presented the result that adjusted the data with an RMS error E_m = 1.67 $\times$ 10^{-3} and 3 m deviations for the position, 0.003 s/km for slowness and 6 $\times$ 10^{-4} s for time. The estimated velocity model is illustrated in Figure 3b. For comparison, the exact velocity model is illustrated. The migrated field with the estimated velocity model is illustrated in Figure 4b. The event focus in this image in comparison with the migrated image with the exact model (Fig. 4a) validates the method effectiveness.

APPLICATION TO REAL DATA

Description and data treatment

The seismic line used was the 214-RL-0266 and it was part of a 2D marine seismic acquisition carried out in Jequitinhonha Basin, south of Bahia, in front of the mouth of the Jequitinhonha River. These data were kindly provided by Petrobras for CPGG/UFBA and the format is SEG-Y. The data acquisition parameters are described in Table 1.

Table 1 – Seismic line 214-RL-0266 acquisition parameters.

Parameter description	Parameter used
Spread (m)	0-150-3125
Interval between receivers (m)	25
Interval between shots (m)	25
Number of shots	1577
Number of channels	120
Sampling interval (ms)	4
Number of samples	1751
Record time (s)	7,00
Shortest offset (m)	150
Largest offset (m)	3125

An important part in the seismic data processing is the identification and the subsequent elimination of the multiple

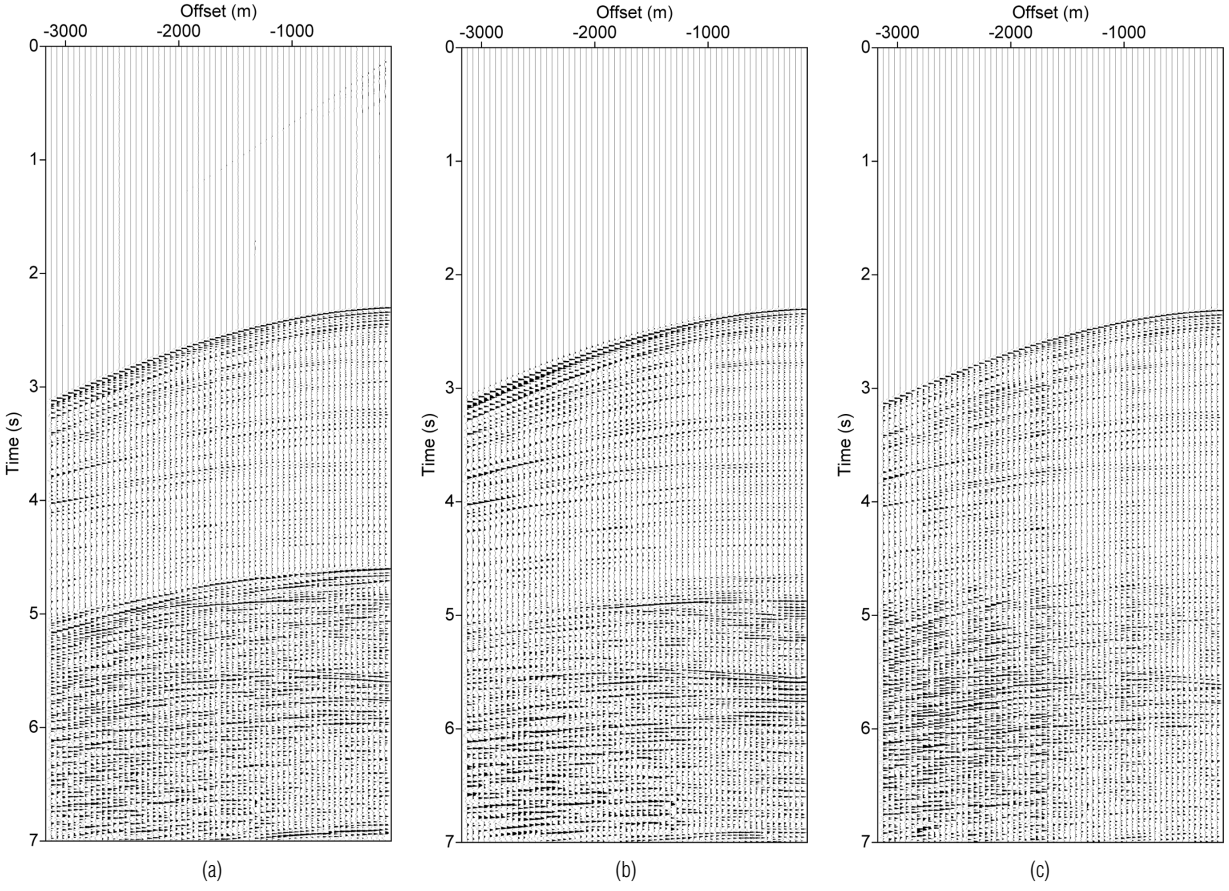

Figure 5 – Comparison between: (a) input data, (b) multiples attenuated by the SRME and Radon methods, and (c) multiples attenuated by the Morf and SRME methods.

reflections. The interference of multiple energy with primary events results in a distorted representation of the subsurface and introduces interpretation uncertainties. And in the event (essentially primaries) selection step of the stereotomography, it is indispensable to have the multiple events attenuated, so that they are not mixed up with the primary events. Then, different from the numeric example presented, we applied some methods to attenuate the multiples, mainly those related to the sea floor. After some tests, two methodologies were selected to attenuate the multiples: the first, conjugating the SRME and Radon methods, and the second, conjugating the methods with Morf filter and SRME. The methodologies were very effective, although the amplitudes were better preserved and also for longer time intervals by the SRME and Radon methodology. The results can be observed in Figure 5.

Application of stereotomography

The method was applied to various pick sets. For illustration, the applications to two pick sets, regarding two processing flow for multiple attenuation, were chosen. The first uses a conjugation of the SRME and Radon methods. In turn, the second employs a conjugation of the Morf filter and SRME methods. It is worth noting that, in this case, the selection of the best pick set was not defined based only on the quality control offered by the tool, the inversion result was also used as a quality control criterion. The scatter point distribution in the estimated velocity model allowed identifying anomalous picks which were eliminated in a subsequent inversion.

The first pick set is formed by 19442 events, that is, 19442 pairs of ray segments and slowness values, being the picking acceptance criterion a semblance value above 0.7. Besides, during the quality control, 28% of the picks were discarded, totalizing 5362 removed events and 14080 used events. With the same semblance criterion, only 8173 picks were collected for the second set and 93% were used effectively, that is, 7609 events were selected during the quality control for the inversion step. This difference reflects the poorer effectiveness of the first processing flow for the multiple elimination (SRME + Radon). Consequently, more spurious events associated to

multiples that were not completely removed are selected. The purpose of using the same criteria for the event selection was to highlight the importance of the multiple elimination flow for the picking step.

For the stereotomographic inversions with a sparse grid, the initial model was defined by a homogeneous velocity field described by 100 nodes, with 5 km lateral spacing and 1 km vertical spacing. For the dense grid, the model used for the inversions was formed by 21 $\times$ 19 nodes, with 2.5 km lateral spacing and 0.5 km vertical spacing, from B-spline interpolation.

The final velocity model, presented in Figures 6a, 6c and 6e for the first pick set and in Figures 6b, 6d and 6f for the second, was obtained after 100 linear iterations and it was described by a total of 4101 $\times$ 1001 nodes and with a final sampling of 10 m laterally and 5 m vertically. The estimated model for the first pick set presents RMS error E_m = 4.07 $\times$ 10^{-2} and 5 m deviations for the position, 0.076 s/km for slowness and 2 $\times$ 10^{-4} s for time, whereas the second set presents RMS error E_m = 3.64 $\times$ 10^{-3} and 4 m deviations, 0.068 s/km and 1 $\times$ 10^{-4} s. These results corroborate the more effectiveness of the second processing flow for the multiple elimination. That is, there is a larger quantity of events associated to multiples in the first pick set.

In general, the results presented a good spatial reflection point distribution, except in the shallow part, where the picks do not clearly define the reflector continuity, as we can observe in Figures 6c and 6d. In the deeper part, for example, as Figures 6e and 6f show, it is possible to clearly observe the continuity of some reflectors. In these figures too, we can state that the second pick set (Fig. 6f) was the best adjusted set in relation to event continuity (sea floor, for example) in comparison with the first set (Fig. 6e).

Finally, we present in Figures 7 and 8 the section migrated in depth, using the stereotomography final velocity model for the first and second pick sets, respectively. The migrated sections confirm the quality of the velocity model estimated by the stereotomography, mainly in the slope region and in the deeper part, where the ray coverage is relatively high and the picks present a higher coherence, resulting consequently in a better velocity estimation. It is even possible to note that the velocity model estimated with the second processing flow for multiple attenuation provides a migrated section with a larger quantity of events in the slope region. The used migration method was implemented by Amazonas et al. (2007), who used finite-difference migration using complex Padé approximations in prestack data.

CONCLUSIONS

The slope tomography formulated by Billette & Lambaré (1998) proved to be efficient to estimate a velocity macro-model in real data, acquired in slope regions. The application to real data requires a careful and effective processing flow for coherent noise attenuation, an efficient automatic picking tool to detect locally coherent events, and quality control of the selected events. This preprocessing flow together with a robust inversion algorithm allowed estimating velocity models that produced images focused in depth.

In this work we present a stereotomography implementation with additional regularization alternatives (Costa et al., 2008). Before the application to real data, this modified algorithm was successfully validated in the Marmousoft synthetic data set (Billette et al., 2003).

Surely, picking, in stereotomography, is the most difficult problem for application to real data. In this step, a human intervention is further necessary. So, the adopted strategy was the rigorous pick quality control, not only based on the selection tool quality control, but also on the inversion result, where it is easy to observe the possible scatter points (picks) that were not correctly adjusted and are then inconsistent with the estimated velocity model.

Although the strong presence of coherent noise in the used data, particularly the short period multiples in the continental shelf region, and the free surface multiples in the continental slope region, the combination of the SRME and Morf methods allowed selecting events associated mainly to primary reflections. The other crucial step for an effective algorithm application is the selection of the regularization parameters that control the smoothness degree of the estimated velocity model. In this work, these parameters were selected from various numeric experiments for different parameter values. The velocity model estimated with this strategy produced focused events in depth, particularly in the slope region and in the deep water region. In the continental shelf region, the image quality improvement still requires a better attenuation strategy for the short period multiples.

ACKNOWLEDGMENTS

The authors would like to thank Frédéric Billette, Gilles Lambaré and Pascal Podvin for providing the availability of the picking program and Marmousoft data, to the geophysicists of PETROBRAS Manoel Gontijo and Ricardo Cruz, who helped in the multiple attenuation step, to FINEP for the Rede CT-PETRO de Geofísica de Exploração – Rede 01 – Fase 3 “Imageamento do Talude

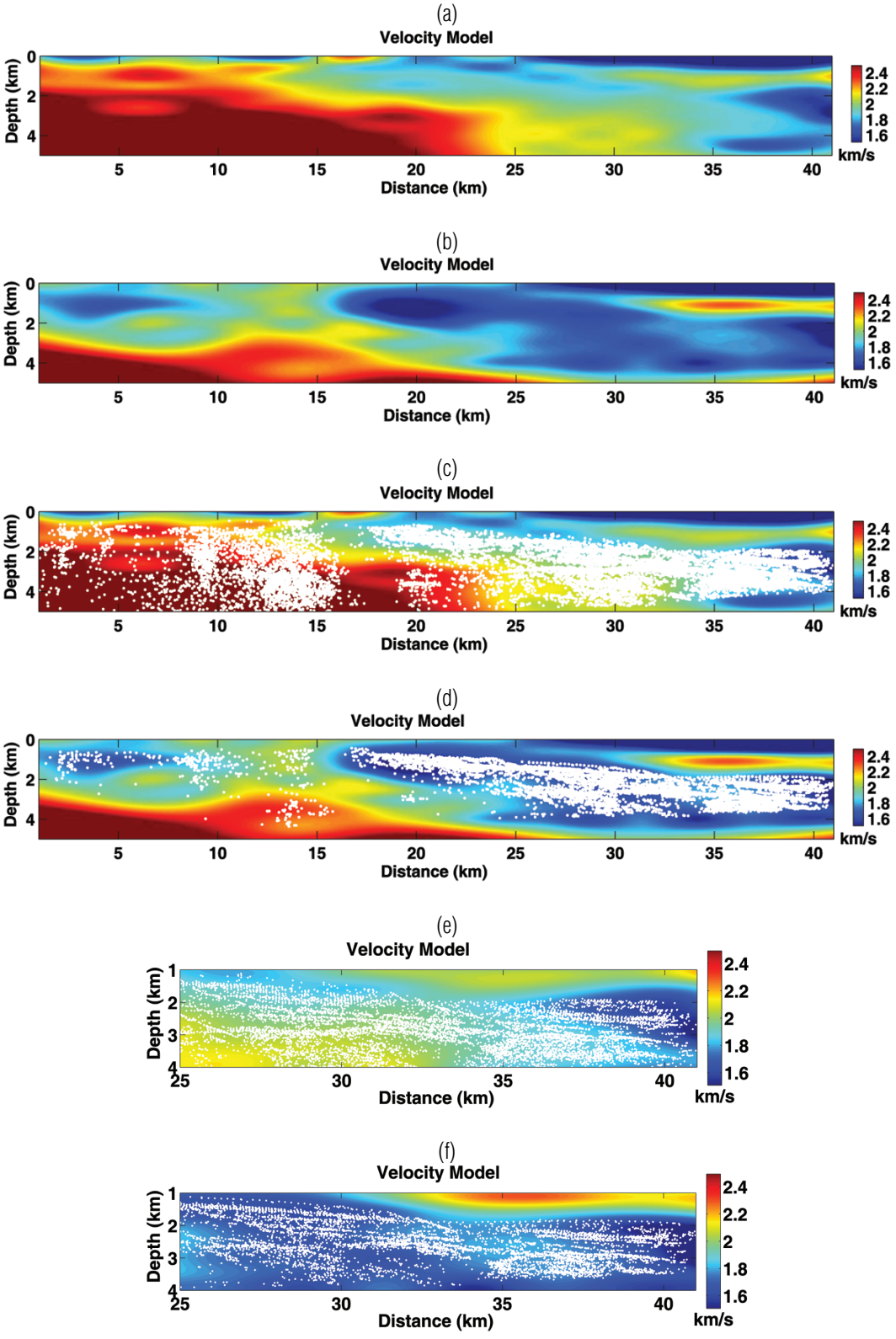

Figure 6 – (a) Estimated velocity model with the multiples attenuated by the SRME and Radon methods. (b) Estimated velocity model with the multiples attenuated by the Morf and SRME methods. (c) Selected picks in the estimated velocity model with the multiples attenuated by the SRME and Radon methods. (d) Selected picks in the estimated velocity model with the multiples attenuated by the Morf and SRME methods. (e) Detail of Figure 6c. (f) Detail of Figure 6d.

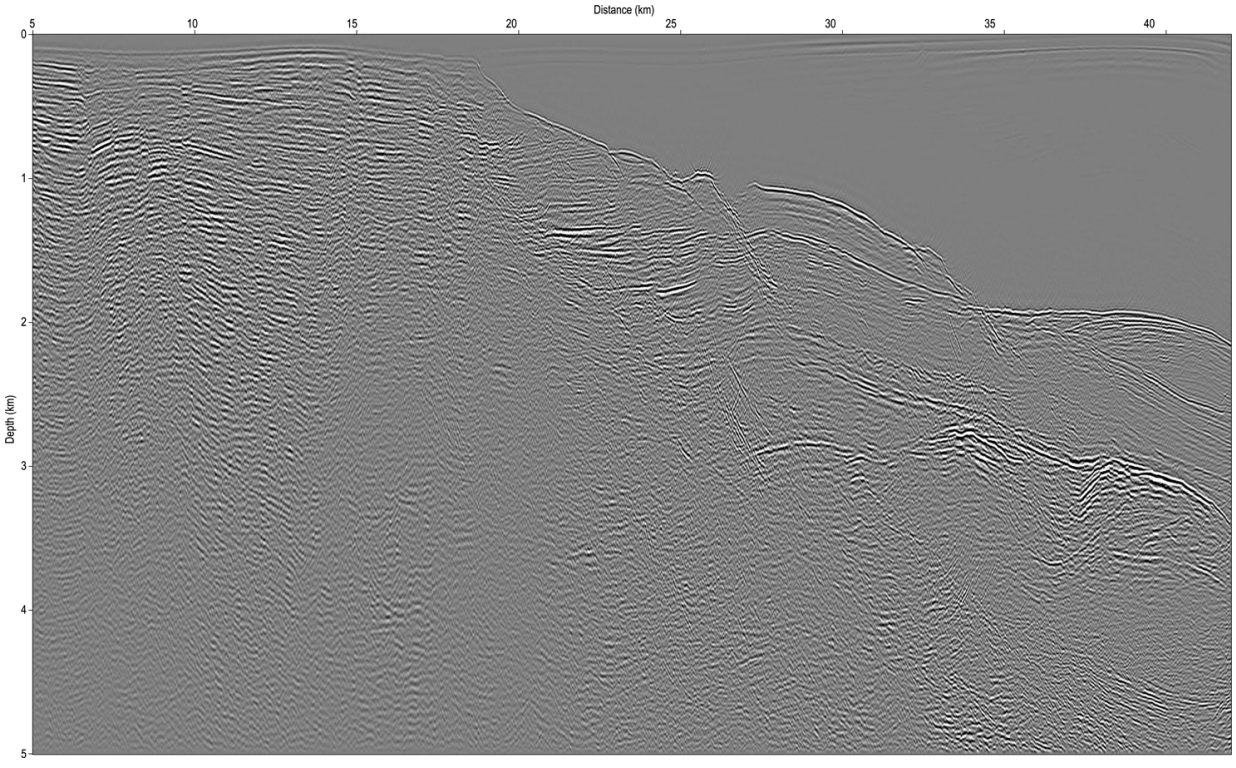

Figure 7 – Migrated seismic session with the estimated velocity model with the multiples attenuated by the SRME and Radon methods.

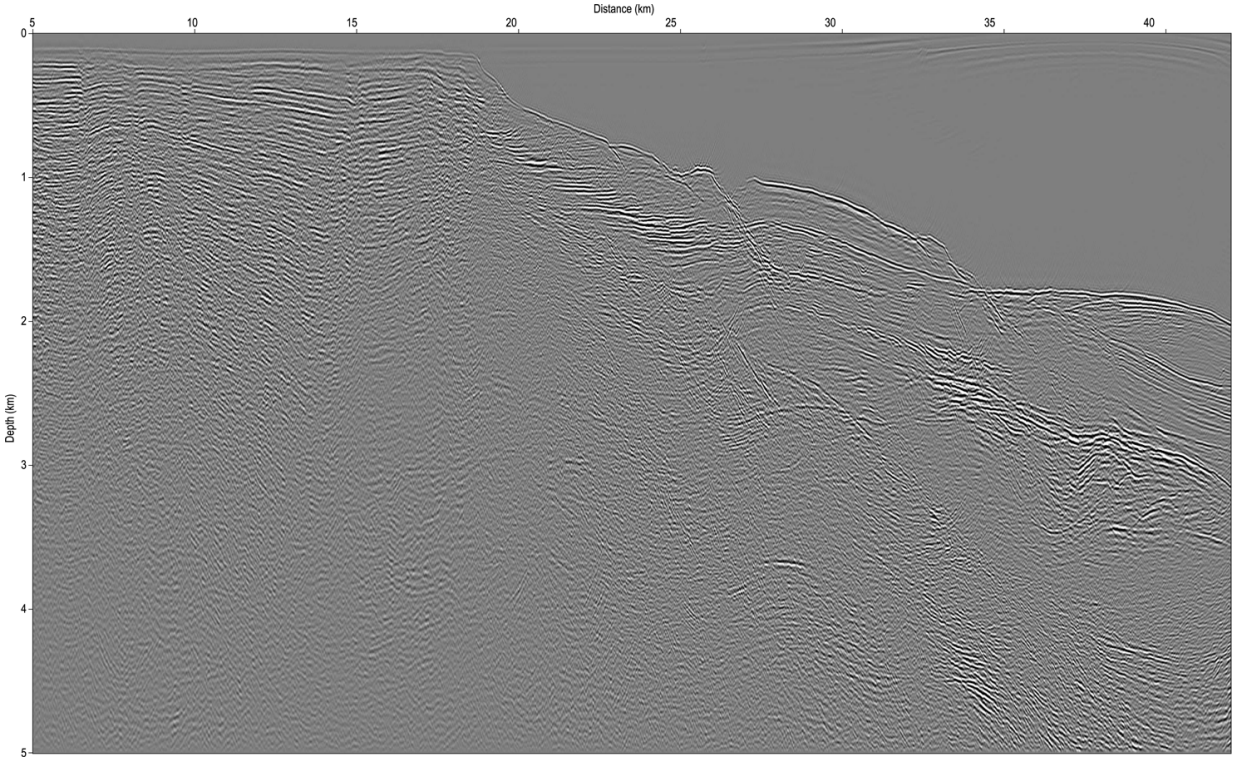

Figure 8 – Migrated seismic session with the estimated velocity model with the multiples attenuated by the Morf and SRME methods.

Continental" support, to PETROBRAS for providing real data, and to LAGEP/CPGG/UFBA for the computational resources. Felipe Terra would like to thank CNPq and ANP/PRH-08 for the master degree scholarship. Amin Bassrei and Jessé Costa would like to thank CNPq for the research productivity scholarship.

REFERENCES

ANDERSON WLO. 1989. A hybrid fast Hankel transform algorithm for electromagnetic modeling. Geophysics, 54: 263–266.

AMAZONAS DR, COSTA JC, SCHLEICHER J & PESTANA R. 2007. Wide-angle FD and FFD migration using complex Padé approximations. Geophysics, 72: S215–S220.

BILLETTE F & LAMBARÉ G. 1998. Velocity macro-model estimation from seismic reflection data by stereotomography. Geophysical Journal International, 135: 671–690.

BILLETTE F, LE BEGÁT S, PODVIN P & LAMBARÉ G. 2003. Practical aspects and applications of 2D stereotomography. Geophysics, 68: 1008–1021.

CERVENÝ V, MOLOTKOV IA & PSENCIK I. 1977. Ray theory in seismology: Charles University Press, Praha. 214 pp.

COSTA JC, SILVA FJC, GOMES ENS, SCHLEICHER J, MELO A & AMAZONAS D. 2008. Regularization in slope tomography. SEG Technical Program Expanded Abstracts, 27(1): 3325–3329.

FARRA V & MADARIAGA R. 1987. Seismic waveform modeling in heterogeneous media by ray perturbation theory. Journal of Geophysical Research, 92: 3697–2712.

LAMBARÉ G, LUCIO PS & HANYGA A. 1996. Two-dimensionalmulti-valued traveltime and amplitude maps by uniform sampling of ray field. Geophysical Journal International, 125: 584–598.

PAIGE C & SAUNDERS MA. 1982. LSQR: Sparse linear equations and least squares problems. ACM Trans. Math. Soft., 8: 43–71.

SWORD CH. 1986. Tomographic determination of interval velocities from picked reflection seismic data. In: 56th Annual SEG Meeting and Exposition, Society of Exploration Geophysicists, pages 657–660.

TARANTOLA A. 1987. Inverse problem theory: Methods for data fitting and model parameter estimation. Elsevier. 613 pp.

NOTES ABOUT THE AUTHORS

Felipe Antonio Terra holds a B.Sc. degree in Geophysics (2007) and an M.Sc. in Geophysics (2010), both from the Federal University of Bahia. He is a geophysicist at PETROBRAS since 2008. He has experience in Geophysics in the following topics: seismic processing, seismic inversion, seismic tomography, velocity analysis and seismic migration.

Jessé Carvalho Costa holds a B.Sc. in Physics (1983), an M.Sc. in Geophysics (1987) and a D.Sc. degree in Geophysics (1994), all from the Federal University of Pará (UFPA). He did the post-doctoral training at Stanford University. He is currently Associate Professor IV at the Faculty of Geophysics at UFPA. He is a member of the Managing Committee of the National Institute of Science and Technology in Petroleum Geophysics (INCT-GP). He has experience in Geophysics in the following topics: wave propagation in anisotropic media, seismic imaging and seismic tomography.

Amin Bassrei holds a B.Sc. degree in Electrical Engineering (1985) and a D.Sc. degree in Geophysics (1990), both from the Federal University of Bahia (UFBA). He did the post-doctoral training in Petroleum Geophysics at the MIT's Earth Resources Laboratory. He is currently Associate Professor IV at the Department of Geophysics at UFBA. He is coordinator of the postgraduate program in Geophysics at UFBA. He is coordinator of the Research Network in Exploration Geophysics (FINEP). He has experience in Geophysics in the following topics: inverse problems, seismic tomography, signal analysis, potential methods, and geological storage of CO_2.